Journal of Immunological Methods 473 (2019) 112633

Contents lists available at ScienceDirect

Journal of Immunological Methods

journal homepage: www.elsevier.com/locate/jim

Research paper

Expression, purification, and characterization of a human complement component C3 analog that lacks the C-terminal C345c domain

Kasra X. Ramyar[a,1], Xin Xu[a,1], Natalie M. White[a], Andrew Keightley[b], Brian V. Geisbrecht[a,*]

[a] Department of Biochemistry & Molecular Biophysics, Kansas State University, 141 Chalmers Hall, 1711 Claflin Road, Manhattan, KS 66506, United States of America
[b] School of Biological Sciences, University of Missouri-Kansas City, 5100 Rockhill Road, Kansas City, MO 64110, United States of America

ARTICLE INFO

Keywords:
Complement system
Complement component C3
Stable cell line
Proteolysis
TEV protease
Surface Plasmon Resonance

ABSTRACT

The complement system consists of a series of soluble and cell-surface proteins that serve numerous roles in innate immunity, development, and homeostasis. Despite its many functions, the central event in the complement system is the proteolytic activation of the 185 kDa complement component 3 (C3) into its opsonin and anaphylatoxin fragments known as C3b (175 kDa) and C3a (10 kDa), respectively. The C3 protein is comprised of thirteen separate structural domains, several of which undergo extensive structural rearrangement upon activation to C3b. In addition to this, the C-terminal C345c domain found in C3, C3b, and the terminal degradation product, C3c (135 kDa), appears to adopt multiple conformations relative to the remainder of the molecule. To facilitate various structure/function studies, we designed two C3 analogs that could be activated to a C345c-less, C3c-like state following treatment with Tobacco Etch Virus (TEV) protease. We generated stably transfected Chinese Hamster Ovary (CHO) cell lines that secrete approximately 1.5 mg of the highest-expressing C3 analog per liter of conditioned culture medium. We purified this C3 analog by sequential immobilized metal ion affinity and size exclusion chromatographies, activated the protein by digestion with TEV protease, and purified the resulting C3c analog by a final size exclusion chromatography. The conformations and activities of our C3 and C3c analogs were assessed by measuring their binding profiles to known C3/b/c ligands by surface plasmon resonance. Together, this work demonstrates the feasibility of producing a C3 analog that can be site-specifically activated by an exogenous proteolytic enzyme.

1. Introduction

The complement system is an essential component of the human innate immune response, wherein it serves important roles in the detection and destruction of foreign organisms, recruitment of phagocytic cells, and clearance of immune complexes among others (Ricklin et al., 2010). Furthermore, recent work has expanded our understanding of the diverse contributions of complement to development, homeostasis, and inflammatory and degenerative diseases such as cancer and Alzheimer's Disease (Ricklin and Lambris, 2013; Hajishengallis et al., 2017). Consisting of some 30 unique soluble and cell-surface retained proteins, the complement system can be triggered by three canonical routes known as the Classical, Lectin, and Alternative Pathways (Ricklin et al., 2010). Although the biochemical stimulus for initiating each of these pathways differs considerably, all three pathways converge at the level of activating the third component of complement, commonly known as C3 (185 kDa), into its C3b (175 kDa) and C3a (10 kDa) fragments (Ricklin et al., 2010; Sahu and Lambris, 2001; Ricklin et al., 2016). Whereas the C3a fragment exhibits physiological properties of an anaphylatoxin, the C3b fragment becomes covalently linked to nearby surfaces. C3b functions in this context as both an opsonin and hub for various protein-protein interactions that drive downstream processes within the complement system (Ricklin et al., 2010; Sahu and Lambris, 2001; Ricklin et al., 2016).

Under normal circumstances, C3 becomes activated through site-specific proteolytic cleavage by transiently stable, multi-subunit serine proteases known as C3 convertases (Ricklin et al., 2010, 2016; Sahu and Lambris, 2001). C3 convertase assembly occurs in a step-wise fashion and proceeds through the initial association of a pro-protease zymogen with a platform molecule, followed by cleavage into a fully active enzyme complex. The Classical and Lectin Pathways share a C3 convertase that forms when the zymogen C2 binds to the surface-linked platform molecule, C4b, and becomes activated by cleavage of C4b/C2 into C4b/C2a. Similarly, the Alternative Pathway C3 convertase forms when the

* Corresponding author.
E-mail address: GeisbrechtB@ksu.edu (B.V. Geisbrecht).
[1] These two authors contributed equally to this work.

https://doi.org/10.1016/j.jim.2019.07.005
Received 15 May 2019; Received in revised form 27 June 2019; Accepted 11 July 2019
Available online 15 July 2019
0022-1759/

zymogen factor B (B) binds to the surface-linked component, C3b, and becomes activated via cleavage of C3b/B into C3b/Bb. It is the Alternative Pathway C3 convertase that is responsible for the remarkable self-amplifying nature of the complement system, as it contributes greater than 80% of the complement activation products generated under physiological conditions (Harboe et al., 2004). Moreover, the convertase-mediated deposition of increasingly greater levels of C3b on surfaces causes a change in the substrate specificity of both convertases from C3 to C5 (Rawal and Pangburn, 2000, 2001, 2003). Proteolytic activation of C5 into C5a and C5b represents the final enzymatic step in the complement system. It also sets the stage for key effector functions of complement, including the recruitment of phagocytic cells to the site of complement activation (via C5a) and formation of the terminal complement complex (via C5b) (Ricklin et al., 2010, 2016; Sahu and Lambris, 2001).

The structures of human C3 (Janssen et al., 2005), as well as its activation products C3b (Janssen et al., 2006) and C3c (Janssen et al., 2005), have been extensively characterized by X-ray crystallography (Gros et al., 2008). This work has revealed that activation of C3 into C3b involves global conformational changes that serve to both create and destroy the various ligand binding sites responsible for the divergent functional properties of C3 and C3b (Fig. 1A). Most notably, while the eight macroglobulin-like domains that comprise the so-called "key ring" of C3 remain essentially static, both the CUB (for Complement C1r/C1s, Uegf, and Bmp1) and TED (for thioester-containing) domains undergo a large rotation and translation relative to the remainder of the molecule. One important consequence of this change is creation of a portion of the C3b binding site for the Alternative Pathway zymogen, fB (Forneris et al., 2010). Subsequent degradation of C3b to C3c through the proteolytic activity of factor I in the presence of factor H removes the CUB-TED region, destroys this aspect of the fB binding site, and renders C3c incapable of interaction with fB. The remainder of the fB binding site is derived from the C345c domain (Forneris et al., 2010). Although the C345c domain does not experience dramatic positional changes when compared to the CUB-TED region, the short linker which connects C345c to the key ring appears partly capable of rotating around the axis defined by the longest dimension of the C3/b/c structure. Indeed, since the C345c domain appears to contribute the only binding site on C3b for Bb, such rotations have been proposed as critical for efficient proteolytic cleavage of substrate by the Alternative Pathway C3 convertase (Rooijakkers et al., 2009).

Although the C345c domain is required for interactions with fB, several other ligand binding sites exist on C3/b/c that either have already been shown or appear capable of functioning in the absence of C345c. Among these are the complement receptor CRIg (Wiesmann et al., 2006) and the synthetic inhibitor Compstatin (Janssen et al., 2007), which recognize the sites on the key ring of C3b, as well as the complement regulatory proteins fH (Wu et al., 2009; Kajander et al., 2011) and *S. aureus* Efb-C (Hammel et al., 2007a) and Ehp (Hammel et al., 2007b), all of which interact with sites on the TED domain. Separately, the intrinsic flexibility of the C345c domain may present a practical barrier to generating protein crystals capable of diffracting X-rays to as high a resolution that might otherwise be achievable. This has hampered the ability to study inhibitory small molecules bound to various C3/b/c sites independent of the C345c domain (Garcia et al., 2017). Therefore, to provide a route for structural and functional study of C3 and its derivatives in the absence of the C345c domain, we designed two analogs of human C3 that could be activated to a C345c-less, C3c-like state following treatment with Tobacco Etch Virus (TEV) protease. Here we describe the methods employed and results of these efforts, as well as the biochemical characterization of a recombinant analog of human C3 lacking its C345c domain in both the C3– and C3c-

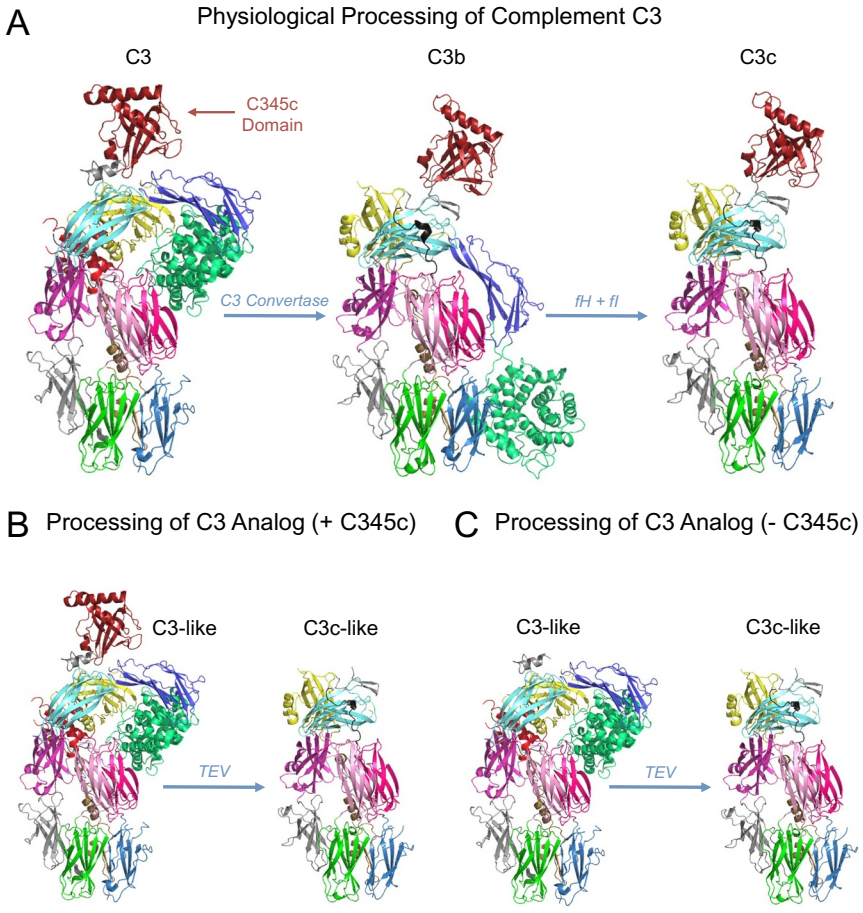

Fig. 1. Structural representation of the activation and degradation of human complement component C3 and two recombinant analogs.
(A) Structural representation of native C3, its activation into C3b via proteolysis by a C3 convertase, and the degradation of C3b into C3c via the activities of fH and fI. Images were drawn using PyMol from PDB entries 2A73 (Janssen et al., 2005, 2006, 2007), and 2A74 (Janssen et al., 2005), respectively. (B) Structural representation of a human C3 analog containing the C345c domain, followed by its activation by TEV protease to a C3c-like state that lacks the C345c domain. (C) Structural representation of a human C3 analog expressed without the C345c domain, followed by its activation by TEV protease to a C3c-like state. The images in panels B and C were drawing using PyMol from the PDB entries 2A73 (Janssen et al., 2005) and 2A74 (Janssen et al., 2005), respectively.

like states.

2. Methods

2.1. Molecular biology and plasmid construction

The coding sequence for each human C3 analog was assembled from a series of GeneBlock synthetic designer gene fragments (Integrated DNA Technologies, Coralville, IA) that had been individually subcloned into pBluescript II SK (+) and sequence confirmed. Following complete assembly of the human C3 analog sequences, the corresponding inserts were directionally subcloned into the mammalian cell expression vector pCI-neo with *Nhe*I and *Not*I sites at the 5′- and 3′-ends, respectively. The coding sequence and translation product for each human C3 analog is provided as supporting information (Fig. S2). All plasmids were purified by isopyncic density gradient centrifugation over CsCl prior to use in cell culture applications.

2.2. Cell lines, transfection, selection, and amplification

A Chinese Hamster Ovary (CHO) cell line deleted for the gene encoding dihydrofolate reductase (*dhfr* −/−) was chosen for generating stably transfected mammalian cells expressing both human C3 analogs. All procedures involving routine culturing and maintenance of these cells, transfection by electroporation, and selection of stable transfectants were performed as described by Leahy and coworkers (Leahy et al., 2000). Amplification of protein expression was carried out by culturing precursor cells in increasingly higher concentrations of methotrexate as previously described (Leahy et al., 2000), with the exception that clonal populations of cells were isolated using 3.2 mm Bel-Art sterile paper cloning disks according to manufacturer's suggestions. Protein expression levels of individual clones were assessed by immunoblotting conditioned culture medium after 2–4 days of growth using either (i) an HRP-conjugated anti-human C3 goat IgG (MP Biomedicals) or (ii) a rabbit antibody recognizing human C3a (Calbiochem) followed by a goat anti-rabbit HRP conjugate (ThermoFisher).

Stably transfected CHO cell lines expressing the highest levels of human C3 analog were expanded into twenty 175-cm^2 vented flasks and cultured at 37 °C in a humidified incubator containing 5% (*v*/v) CO_2 in the atmosphere. Cells were maintained in a medium consisting of DMEM High Glucose (Corning cellgro number 10–013-CM) supplemented with 1% (v/v) Bovine Calf Serum, 1% (v/v) Non-Essential Amino Acids solution (HyClone number SH30238.01), and 1% (v/v) of a penicillin/streptomycin solution. The medium in all flasks was exchanged every 3–4 days. Conditioned culture medium was centrifuged following collection (20,000 × *g* for 30 min) to remove cell debris and precipitated materials, and stored at 4 °C until further use. Pilot experiments were also carried out using PowerCHO-3-CD serum free medium (Lonza Catalog Number 12-772Q) in place of DMEM High Glucose.

2.3. Protein expression and purification

Purification of the human C3 analog lacking the C345c domain was achieved through sequential immobilized metal ion affinity and size-exclusion chromatographies carried out at room temperature on a GE Life Sciences AKTA pure FPLC system. Briefly, 2 L of clarified conditioned culture medium was concentrated ten-fold using a Millipore lab-scale tangential flow filtration device equipped with 30 kDa nominal molecular weight cut-off filters. The buffer of the concentrated sample was exchanged to 20 mM tris (pH 8.0), 500 mM NaCl, 10 mM imidazole (pH 8.0) according to the manufacturer's suggestions. Following clarification by 0.45 μm filtration, the exchanged sample was applied at a flow rate of 4 ml/min to a 5 ml HiTrap Chelating column (GE Life Sciences) that had been previously charged with 100 mM $NiSO_4$ and equilibrated in the sample buffer. The column was washed extensively with sample buffer, prior to eluting the bound proteins at a flow rate of 2 ml/min with a linear gradient over 7.5 column volumes to 20 mM tris (pH 8.0), 500 mM NaCl, 500 mM imidazole (pH 8.0) while collecting 2 ml fractions. Fractions containing human C3 analog (as judged by SDS-PAGE performed under non-reducing conditions) were pooled and injected at a flow rate of 4 ml/min onto a Superdex S200 26/60 size exclusion chromatography column (GE Life Sciences) that had been previously equilibrated in phosphate-buffered saline (pH 7.4). Fractions of the column eluate (2 ml each) were collected and analyzed by SDS-PAGE performed under non-reducing conditions. Fractions containing the human C3 analog were pooled, concentrated by ultrafiltration, and stored at 4 °C for further use.

2.4. Proteolytic activation of the human C3 Analog

The purified human C3 analog was activated by site-specific digestion with TEV protease fused to the C-terminus of *E. coli* maltose-binding protein. MBP-TEV was added to the purified substrate at a 1: 50 mass ratio in PBS (pH 7.4). The reaction was allowed to proceed at 37 °C for approximately 48–72 h until it reached completion, as judged by SDS-PAGE performed under non-reducing conditions. Following activation, the human C3c analog was separated from the MBP-TEV fusion protease and other digestion products by size exclusion chromatography. The sample was injected at 0.5 ml/min onto a Superdex S200 10/300 GL column that had been previously equilibrated in PBS (pH 7.4) and fractions of the eluate (1 ml each) were collected. Fractions containing purified human C3c analog were pooled, concentrated by ultrafiltration, and stored at 4 °C until further use.

2.5. Protein characterization by mass spectrometry

Samples of purified proteins were separated by SDS-PAGE performed under non-reducing conditions and stained with Coomassie blue. Excised gel bands corresponding to each sample were reduced, alkylated, and processed for in-gel trypsin digestion by standard methods (Keightley et al., 2004). The extracted peptides were characterized by tandem mass spectrometry according to the methods described by Keightley and coworkers (Keightley et al., 2004). Identification of the C3 and C3c analogs was performed using Mascot 2.4 (Matrix Science) with semi-trypsin specificity.

2.6. Surface Plasmon Resonance studies of ligand binding profiles

The ligand binding profiles of the human C3 and C3c analogs were compared qualitatively to those of purified human C3b and C3c (Complement Technologies, Tyler, TX) by Surface Plasmon Resonance (SPR) as a means of assessing the conformational state of both recombinant proteins. All experiments were performed at 25 °C on a Biacore T-200 instrument (GE Healthcare) at a flow rate of 30 μl/min and utilized a running buffer of HBS-T (20 mM HEPES (pH 7.4), 140 mM NaCl, and 0.005% (*v*/v) Tween-20). Experimental surfaces were prepared on a CMD200 sensor chip (Xantec Bioanalytics GmbH, Dusseldorf, Germany) by immobilizing the *S. aureus* complement inhibitor Efb-C (Hammel et al., 2007a), its inactive mutant Efb-C-RENE (Hammel et al., 2007a) (approximately 1200 RU each), and purified human complement factor H (Complement Technologies, Tyler, TX) (1384 RU) on separate flow cells using random amine chemistry. A reference surface was prepared by immediately injecting ethanolamine over a separate flow cell following activation. Five different samples of either native human C3b, the C3 analog, or its C3c counterpart representing a five-fold dilution series (625 nM maximum) were injected in ascending order of concentration over the surfaces for 2 min with a 1 min dissociation between injections, followed by a single 30 min dissociation phase following the final injection. Regeneration to baseline was obtained by three consecutive 30 s injections of 0.1 M glycine (pH 1.5). All reference-subtracted injection series were analyzed using a

heterogenous ligand binding model (Biacore T-200 Evaluation Software v3.1).

A similar study was performed by injecting native human C3c, the C3 analog, and its C3c counterpart over a surface consisting of immobilized mouse monoclonal antibody, WM-1 (Whitehead et al., 1981). In this case, while a somewhat lower density of capture ligand was used (639 RU), both the analyte concentration series and regeneration to baseline parameters were identical to those described above. All reference-subtracted injection series were analyzed using a Langmuir kinetic binding model (Biacore T-200 Evaluation Software v3.1).

2.7. Surface Plasmon Resonance experiments for quantitative comparison of affinities

The functional properties of the human C3 and C3c analogs were also compared quantitatively to purified human C3c by measuring binding of the C3/b/c ligand, TRX-4W9A (Garcia et al., 2017), to each protein by SPR. Experimental surfaces were prepared on a CMD200 sensor chip (Xantec Bioanalytics GmbH, Dusseldorf, Germany) by immobilizing C3 analog (2544 RU), C3c analog (1618 RU), and native human C3c (1402 RU) on separate flow cells using random amine chemistry. A reference surface was also prepared as described above. Nine different samples of TRX-4W9A representing a two-fold dilution series (5 μM maximum), as well as buffer alone, were injected in ascending order of concentration over the surfaces for 2 min and allowed to dissociate for 3 min. Regeneration to baseline was obtained by two consecutive 30 s injections of 2 M NaCl. All reference-subtracted injection series were analyzed using both Langmuir kinetic and approach to equilibrium binding models (Biacore T-200 Evaluation Software v3.1). Values describing the various binding parameters from three replicate injection series were pooled to derive mean and standard deviations for each parameter.

3. Results

3.1. Practical considerations for expression vector design

Although it is translated from a single type of mRNA transcript, biogenesis of the matured C3 protein found in human serum is a relatively complex process (Sahu and Lambris, 2001). Following removal of a 22-residue signal peptide upon translocation into the endoplasmic reticulum, the human C3 pro-protein is modified by N-linked glycosylation. It also undergoes cleavage into α and β chains of 110 and 75 kDa, respectively, through the action of a furin family protease. Once separated, these chains are then covalently rebound to each other through formation of a single inter-chain disulfide bond. All told, these two chains give rise to thirteen discrete structural domains in the native C3 molecule (Fig. 1 and Fig. S1) (Janssen et al., 2005).

In addition to this, the native C3 protein contains an unusual isoglutamyl cysteine thioester that forms between the sidechains of Cys-1010 and Glutamine-1013 as part of its eponymous thioester-containing TED domain (numbering based on native C3 pre-pro-protein sequence). This thioester is highly reactive to nucleophilic attack, but is largely protected from access to solvent in the structure of native C3 (Janssen et al., 2005). Nucleophilic attack, be it through groups found on nearby cells, carbohydrates, or proteins, is enabled following activation of native C3 to C3b; this allows for covalent attachment of C3b and its well-known function as a both an opsonin and platform for Alternative Pathway C3 convertase assembly. At a structural level, the C3 to C3b conversion is characterized by a massive conformational change that creates what is essentially an entirely different protein in the process (Fig. 1) (Ricklin et al., 2016; Janssen et al., 2006).

Step-wise degradation of C3b is vital to the regulation of complement activity, as the products that result can no longer participate in formation of Alternative Pathway C3 convertases (Ricklin et al., 2010; Sahu and Lambris, 2001). Although several combinations of proteins may play a role in this process, the most common scenario involves factor H-dependent proteolytic cleavage by factor I of the bonds between Arg-1303 and Ser-1304 and Arg-1320 and Ser-1321 producing iC3b, followed by cleavage of the bond between Arg-954 and Glu-955, yielding C3c (Sahu and Lambris, 2001; Xue et al., 2017). Whereas iC3b retains opsonin activity via its interaction with a number of cell-surface exposed complement receptors (Ricklin et al., 2010; Ricklin et al., 2016), C3c has been ascribed no known functions to date. Despite this fact, C3c has proven quite useful as a research tool because this fragment is comprised of the entire key ring region of the C3/b molecule, as well as the C345c domain (Janssen et al., 2005). C3c has therefore found extensive use in structural studies for defining the binding sites of Compstatin (Janssen et al., 2007), CRIg (Wiesmann et al., 2006), and the SCIN family of *S. aureus*-derived complement inhibitors (Garcia et al., 2012; Garcia et al., 2010). Intriguingly, each of these co-crystal structures is characterized by relatively poor model-to-map correlation for the C345c domain. This suggests that the intrinsic dynamics of the C345c domain may negatively influence either the feasibility or quality of crystallographic studies involving C3c.

Our goal was to provide a facile route for mammalian cell expression and purification of a human C3 analog that lacked the flexible C345c domain and which could be activated into a C3c-like state through digestion by an exogenous protease. We incorporated several features in our expression system in the light of the considerations outlined above (Figs. S1 and S2). First, we maintained the signal peptide sequence found in the human C3 pre-pro-protein to direct efficient secretion of the recombinant protein into the culture medium. Second, we eliminated the potential for thioester formation by mutating the thioester cysteine to serine. Third, we incorporated TEV protease recognition sequences to allow for concurrent removal of the C3a domain as well as the entire CUB-TED region. This feature allows for conversion of the C3 analog to a C3c-like state, effectively bypassing the C3b and iC3b forms of the molecule. Fourth, we included a C-terminal octahistidine tag to permit straightforward first-step purification of the target protein from the conditioned culture medium by Immobilized Metal-ion Affinity Chromatography. Finally, we prepared two different expression vectors to accomplish our goal of removing the C345c domain (Figs. S1 and S2). The first of these simply truncated the protein prior to the C345c domain by placement of a stop codon; the second vector included the C345c domain, but replaced several residues N-terminal to this domain with a TEV protease recognition site so that this domain could be removed by site-specific proteolysis. We favored this combined approach in case that lack of the C345c domain might somehow unexpectedly influence expression levels, secretion, or stability of the recombinant C3 protein analogs.

3.2. Generation of stable cell lines expressing analogs of human C3

We used electroporation to co-transfect dihydrofolate reducatase deficient (*dhfr* −/−) CHO cells with a plasmid allowing for constitutive expression DHFR along with plasmids encoding either C3 analog (Leahy et al., 2000). We then selected for stable transfectants by growing the recovering cells in nucleotide-free medium (Leahy et al., 2000) and assayed individual clones for expression of human C3 epitopes by immunoblotting samples of conditioned culture medium. We subjected the highest-expressing cell line for each C3 analog to drug amplification by treatment with increasing concentrations of methotrexate (Leahy et al., 2000). Following two rounds of amplification, we compared the three highest-expressing clones for each C3 analog to one another to determine which cell lines to carry forward for further investigation (Fig. 2).

We found that the anti-C3a immunoreactive band produced by each clone was consistent with expression and secretion of the desired protein product. Moreover, we found that absence of serum did not adversely affect the stability of the either C3 analog, as judged by a lack of obvious change in the apparent molecular weight of the anti-C3a

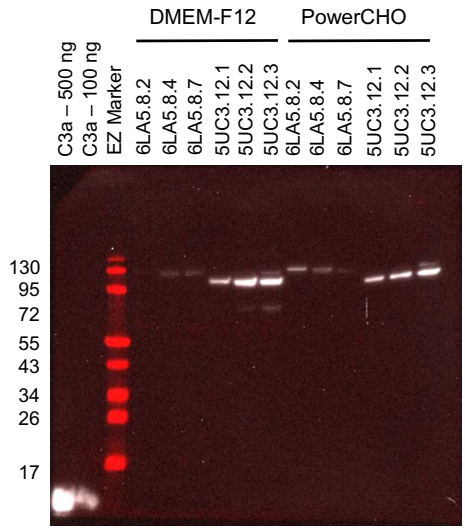

Fig. 2. Characterization of stable CHO cell lines expressing two different human C3 analogs.

Stably transfected CHO cell lines expressing two different human C3 analogs were subjected to methotrexate amplification (Leahy et al., 2000). Individual colonies resulting from amplification were isolated, cultured in either serum-containing (DMEM) or serum-free (PowerCHO) medium, and their supernatants were assayed for the presence of the human C3 analog by immunoblotting against C3a. Colonies expressing the C3 analog that lacked the C345c domain consistently produced higher levels of protein than those expressing the C3 analog with the C345c domain. Note that these samples were prepared under reducing conditions to emphasize the size difference in the α chains of these two different C3 analogs. Two different quantities of purified C3a were included as a control. Sample "EZ" corresponds to Pre-Stained Recombinant Protein Ladder (Fisher Bioreagents). Abbreviations that begin with "6LA5" and "5UC3" refer to individual colonies that were isolated for analysis.

immunoreactive band when the cells were cultured in serum-free versus serum-containing medium. These results strongly suggested that the none of the modifications engineered into the C3 sequence had any globally deleterious consequences on protein stability. Nevertheless, we also observed that all three cell lines expressing the truncated C3 analog produced significantly higher levels of C3 protein than those expressing the full-length C3 analog. Of these, we found that cell lines 5UC3.12.2 and 5UC3.12.3 produced comparably high levels of the truncated C3 analog protein. Thus, we focused our subsequent efforts on large-scale purification and characterization of this molecule.

3.3. Purification of a human C3 analog lacking the C345c domain

We expanded cell line 5UC3.12.3 to large scale culture in T-175 flasks and maintained the cells in DMEM medium supplemented with 1% (*v*/v) bovine serum and non-essential amino acids. We collected the conditioned culture medium every 3–4 days and began purification of the product once 2 L of medium were available. We used tangential flow filtration to concentrate the medium and exchange the buffer in preparation for immobilized metal-ion affinity chromatography by FPLC. We applied the sample to a Ni^{2+}-charged chelating sepharose column and washed extensively to remove unbound contaminants. We then eluted the bound proteins with a linear gradient of imidazole, which generated a large, asymmetric peak (Fig. 3A, B). Analysis of the peak fractions by SDS-PAGE performed under non-reducing conditions revealed the presence of the polyhistidine-tagged human C3 analog in the later-eluting region of this peak (Fig. 3C).

Since the main contaminants in the sample were a doublet of bands of approximately 60 kDa, we opted for further purification by Superdex S200 size-exclusion chromatography. The sample eluted from this column as two main peaks, the latter of which was characterized by

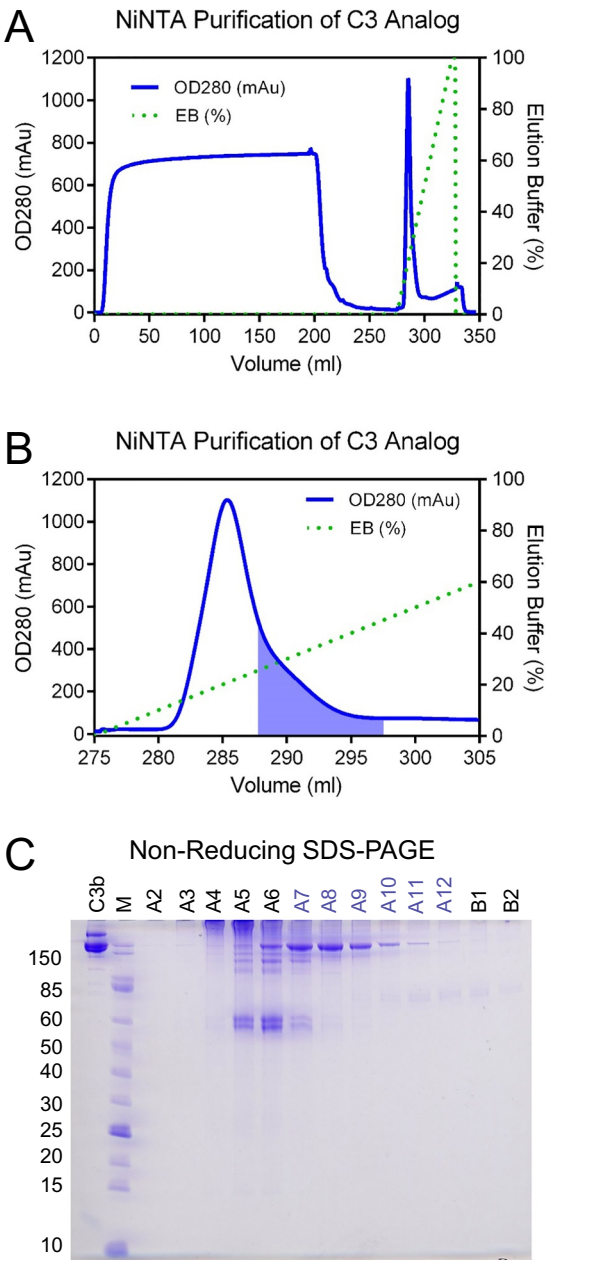

Fig. 3. Initial purification of a human C3 analog by immobilized metal-ion affinity chromatography.

A human C3 analog which lacked the C345c domain was purified by immobilized metal-ion affinity chromatography using 2 L of conditioned culture medium as the starting material. (A) Chromatogram showing elution of protein from the column (left y-axis) along with the relative concentration of elution buffer (right y-axis). (B) Magnified view of the chromatogram shown in panel A, with the fractions selected for pooling and further purification represented by the area shaded in purple. (C) Analysis of column fractions by SDS-PAGE performed under non-reducing conditions. Purified human C3b was included as a control. Lanes representing fractions that were collected for further purification are labeled with purple typeface. Sample "M" corresponds to a broad-range molecular weight standard (New England Biolabs). Names such as "A2", "A3", etc. refer to individual column fractions. (For interpretation of the references to colour in this figure legend, the reader is referred to the web version of this article.)

shoulder that was not well-resolved by this column (Fig. 4A, B). We analyzed the peak fractions by SDS-PAGE performed under non-reducing conditions and found that the later eluting peak contained highly-purified human C3 analog (Fig. 4C). Fractions corresponding to the

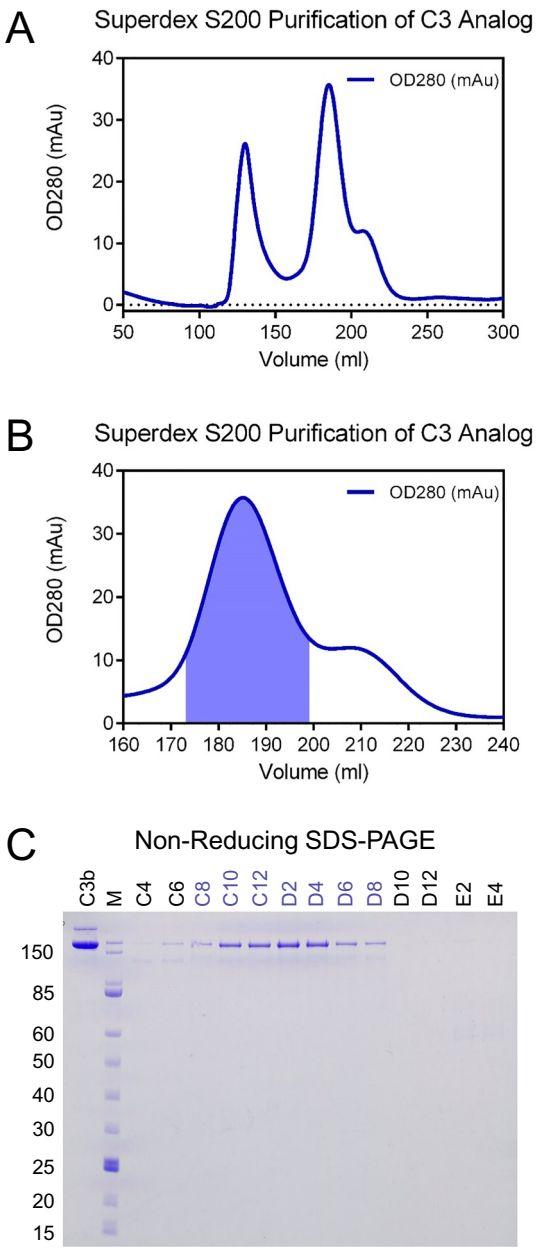

Fig. 4. Final purification of a human C3 analog by size exclusion chromatography.
Fractions from the previous round of affinity chromatography were pooled and further purified by size exclusion chromatography on a Superdex S200 26/60 column. (A) Chromatogram showing elution of protein from the column. (B) Magnified view of the chromatogram shown in panel A, with the fractions selected for pooling represented by the area shaded in purple. (C) Analysis of column fractions by SDS-PAGE performed under non-reducing conditions. Purified human C3b was included as a control. Lanes representing fractions that were collected for further use are labeled with purple typeface. Sample "M" corresponds to a broad-range molecular weight standard (New England Biolabs). Names such as "C4", "C6", etc. refer to individual column fractions. (For interpretation of the references to colour in this figure legend, the reader is referred to the web version of this article.)

center of this peak appeared to be devoid of obvious contaminants, and were therefore pooled and concentrated by ultrafiltration to greater than 1 mg/ml protein. The final yield of purified human C3 analog was approximately 1.5 mg protein per liter of conditioned cultured medium.

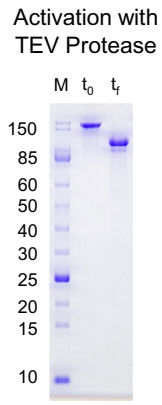

Fig. 5. Activation of a human C3 analog by TEV protease digestion.
The purified human C3 analog was activated to its corresponding C3c-like state by digestion with a TEV protease fusion protein. Samples of both the starting material (t_o) and digestion product following purification by size-exclusion chromatography (t_f) were analyzed by SDS-PAGE performed under non-reducing conditions. Sample "M" corresponds to a broad-range molecular weight standard (New England Biolabs).

3.4. Activation the C3 analog to its C3c-like state by TEV protease digestion

Whereas normal physiological activation of C3 to C3b requires the activity of a C3 convertase, the subsequent conversion of C3b to iC3b and then C3c requires separately the activity of factor I (Fig. 1). By contrast, we designed the truncated human C3 analog to undergo activation to a C3c-like state by incorporating three separate TEV protease sites at positions corresponding to the domain boundaries which define C3a and the CUB-TED region (Fig. 1 and Figs. S1 and S2). We activated the purified human C3 analog by adding a recombinant TEV protease fusion protein (MBP-TEV) at a 1:50 mass ratio and incubating the reaction at 37 °C. Although many recombinant proteins can be cleaved to completion by MBP-TEV within 4–6 h (*our unpublished observations*), we found that the human C3 analog required digestion times of 48–72 h to approach completion. We purified the C3c analog from the remainder of the digestion reaction contents by size-exclusion chromatography and compared the starting material to the purified product (Fig. 5). This revealed a large shift in electrophoretic mobility consistent with theoretical molecular weight of the human C3c analog (~115 kDa).

We used proteomics methods as an independent means to establish the identities of the human C3 analog before and after activation by TEV protease. We prepared tryptic peptides of each sample following in gel digestion, separated the extracted peptides by reversed-phase HPLC, and determined their sequences by tandem mass spectrometry. Peptide coverage for synthetic C3 was approximately 66%, based upon the open reading frame encoded by the truncated human C3 analog expression plasmid (Fig. S3). We observed peptides corresponding to the predicted N-terminus of the protein (i.e. Ser-23) following removal of the signal sequence. We also detected peptides extending both N- and C-terminally from the tetra-arginine site (i.e. Arg-668 to Arg-671, numbering hereafter per the truncated C3 analog pre-pro-protein), but not contiguously through this region. This suggested that the C3 analog protein was correctly processed by a furin-class protease prior to secretion.

By contrast, peptide coverage for the putative human C3c analog decreased to 48% of the plasmid-encoded open reading frame (Fig. S3). Closer inspection of the peptide coverage revealed loss of all peptides corresponding to the C3a region (i.e. Ser-671 to Arg-748), as well as those corresponding to all but the C-terminal extreme of the CUB-TED region (i.e. Gln-940 to Ala-1356). In this regard, we observed seven different peptides covering residues Met-1353 to Lys-1366, which included the TEV protease recognition site from Glu-1357 to Ser-1363. Together, these results suggested that cleavage in this region was not due to TEV protease activity, but rather a result of adventitious

proteolysis by a contaminant present at trace levels in the activation reaction. However, we also found evidence for successful TEV protease digestion at the sites introduced to liberate C3a (i.e. Glu-749 to Ser-755) and at the N-terminal boundary of the CUB domain (i.e. Glu-935 to Gly-941), as judged by the presence of peptides derived from these TEV protease recognition sites in the C3c analog coverage map. When considered together, these proteomic data support our interpretation of the electrophoretic mobility change in the purified product following TEV digestion and confirmed the identify of this product as an analog of human C3c.

3.5. Functional comparison of human C3 and C3c analogs with purified human C3b/c

Although our SDS-PAGE and proteomics data established the identify of the human C3 and C3c analogs at the chemical level, we sought further structural and functional validation of each protein. Since the large conformational changes that accompany C3 activation to C3b are known to create/expose numerous interaction sites that are otherwise unavailable in native C3 (Ricklin et al., 2016; Janssen et al., 2006), the ligand binding profiles of activated forms of C3 vary considerably when compared to the native protein (Sahu and Lambris, 2001; Ricklin et al., 2016; Yang et al., 2013). In the past, we have extensively used SPR to characterize the interactions of complement C3 and its proteolytic activation derivatives with various binding partners (Hammel et al., 2007a; Garcia et al., 2017; Garcia et al., 2012; Ricklin et al., 2009; Summers et al., 2015; Garcia et al., 2013). Consistent with one such report (Hammel et al., 2007a), we confirmed here that native human C3b bound readily to a surface modified with a wild-type form of the staphylococcal innate immune evasion protein Efb-C, but not to a surface modified by a non-functional Efb-C double mutant (Fig. 6A, B). We further determined that native human C3b bound well to a surface derivatized with the endogenous complement regulatory protein, factor H (Fig. 6C). Significantly, we found that the human C3 analog bound only to the wild-type Efb-C surface (Figs. 6D–F). This result strongly suggested that the human C3 analog has a solution conformation more similar to native C3 than to C3b, for while the Efb-C binding site within the TED domain is accessible in native C3 (Hammel et al., 2007a), the factor H binding site only becomes accessible upon activation to C3b (Wu et al., 2009).

Whereas most endogenous biological ligands exhibit selectivity for activated forms of C3 as described above, a number of exogenous interaction partners such as antibodies and peptides fail to display this type of binding preference. Along these lines, the mouse monoclonal antibody WM-1 has been reported to recognize the C3c fragment of the human C3 protein (Whitehead et al., 1981). Although no high-resolution structural information is available regarding the WM-1 binding site on human C3/c, the fact that WM-1 has been used in successful affinity purification of native C3 from serum samples (Dodds, 1993) strongly suggests that the WM-1 epitope remains intact and exposed in C3/b/c. We therefore used a WM-1 derivatized SPR surface to further characterize the solution conformations of our recombinant human C3 and C3c analogs. We found that antibody WM-1 bound similarly to native human C3c (Fig. 6G), as to the C3 (Fig. 6H) and C3c (Fig. 6I) analogs. This result provided further evidence regarding the structural integrity of the recombinant C3 and C3c analog proteins.

Like monoclonal antibody WM-1, the peptidomimetic Compstatin (Katragadda et al., 2006) binds to a site within the “key ring” region that remains constant C3, C3b, and C3c (Janssen et al., 2007). We previously described a protein denoted TRX-4W9A, which consists of *E. coli* thioredoxin fused to a Compstatin variant comprised of entirely natural amino acids (Garcia et al., 2017). TRX-4W9A was previously reported to bind site-specifically immobilized C3b with an equilibrium dissociation constant (K_D) of ~770 nM, as judged SPR (Garcia et al., 2017). Consequently, we prepared biosensors of random-amine immobilized human C3 analog, its C3c analog counterpart, and purified human C3c to characterize the interaction of these proteins with TRX-4W9A (Fig. 7 and Table 1). We found that the C3 and C3c analogs bound TRX-4W9A with K_D values of 956 ± 26 and 1280 ± 96 nM, respectively. These values were in good agreement not only with one another, but with that we determined for purified human C3c as well (1350 ± 8 nM). When considered together, these data confirmed that our analogs of human C3 and C3c maintain proper solution conformations, as well as important functional properties associated with the C3/b/c protein.

4. Discussion

A reliable source of recombinant protein permits a diverse array of structural and functional studies, including isotopic enrichment, incorporation of unnatural amino acids, and site-directed mutagenesis among others. Although prokaryotic expression systems are favored for most applications, many proteins that are normally secreted from human cells (e.g. complement components) require the use of eukaryotic expression hosts such as insect or mammalian cells. These systems allow for extensive post-translational modifications, secretion into the extracellular environment, and may provide a route to production of recombinant proteins that are otherwise unapproachable. We chose CHO cells as our expression host in light of the complex biogenesis of C3 (Fig. 1), and developed a stable cell line that allowed purification of approximately 1.5 mg of a human C3 analog lacking its C345c domain per liter of conditioned culture medium (Figs. 2–4). We showed that this recombinant product could be activated by TEV protease to a C3c-like state following release of both the C3a and CUB-TED regions (Fig. 5). We then carried out a series of comparative SPR experiments to validate the conformational state of this recombinant protein before and after TEV activation. We found that the C3 analog selectively bound to *S. aureus* Efb-C but not complement factor H, consistent with the properties of native human C3 (Fig. 6). We also determined that both the C3 and C3c-like states of the analog bound with high affinity to monoclonal antibody WM-1 (Fig. 6) and the TRX-4W9A fusion protein (Fig. 7), which recognize distinct sites on the C3/b/c protein. Together, our work has demonstrated the feasibility of producing recombinant C3-like molecules that can be activated by an exogenous protease and retain biological function. In the future, we believe that similar approaches could be be useful in answering structural and functional questions on central complement components and their interactions with one another.

Beginning with its initial synthesis as a pre-pro-protein to its terminal physiological degradation to C3c, an individual C3 molecule can undergo six or more different site-specific proteolytic reactions during its lifespan (Sahu and Lambris, 2001). This ordered series of biochemical transformations requires at least five different proteolytic enzymes, as well as their associated cofactors (Sahu and Lambris, 2001). To simplify this process in an in vitro setting, we introduced a series of TEV protease recognition sequences into the C3 pre-pro-protein under the premise that a highly specific exogenous protease might be able to mimic the reactions normally catalyzed by a C3 convertase and fI (Sahu and Lambris, 2001). Proteomic analysis of the purified C3 analog revealed that cleavage of the pre-pro-C3 signal peptide and subsequent processing of the pro-protein into α and β chains occurred as expected (Fig. S3). However, while we found that the purified C3 analog could be successfully activated into its corresponding C3c-like state following TEV digestion (Fig. 5 and Fig. S2B), we also determined that bona fide TEV digestion occurred at only two of the three sites introduced into the C3 analog protein. This raised questions about the why two sites were cleaved efficiently during TEV digestion (i.e. Glu-749 to Ser-755 and Glu-935 to Gly-941), while the third appeared to be resistant (i.e. Glu-1357 to Ser-1363).

We examined the sequence and structures of C3/b/c to gain insight into why TEV cleavage failed at the C-terminal boundary of the CUB-TED region. Even though the sequence we introduced matched the most

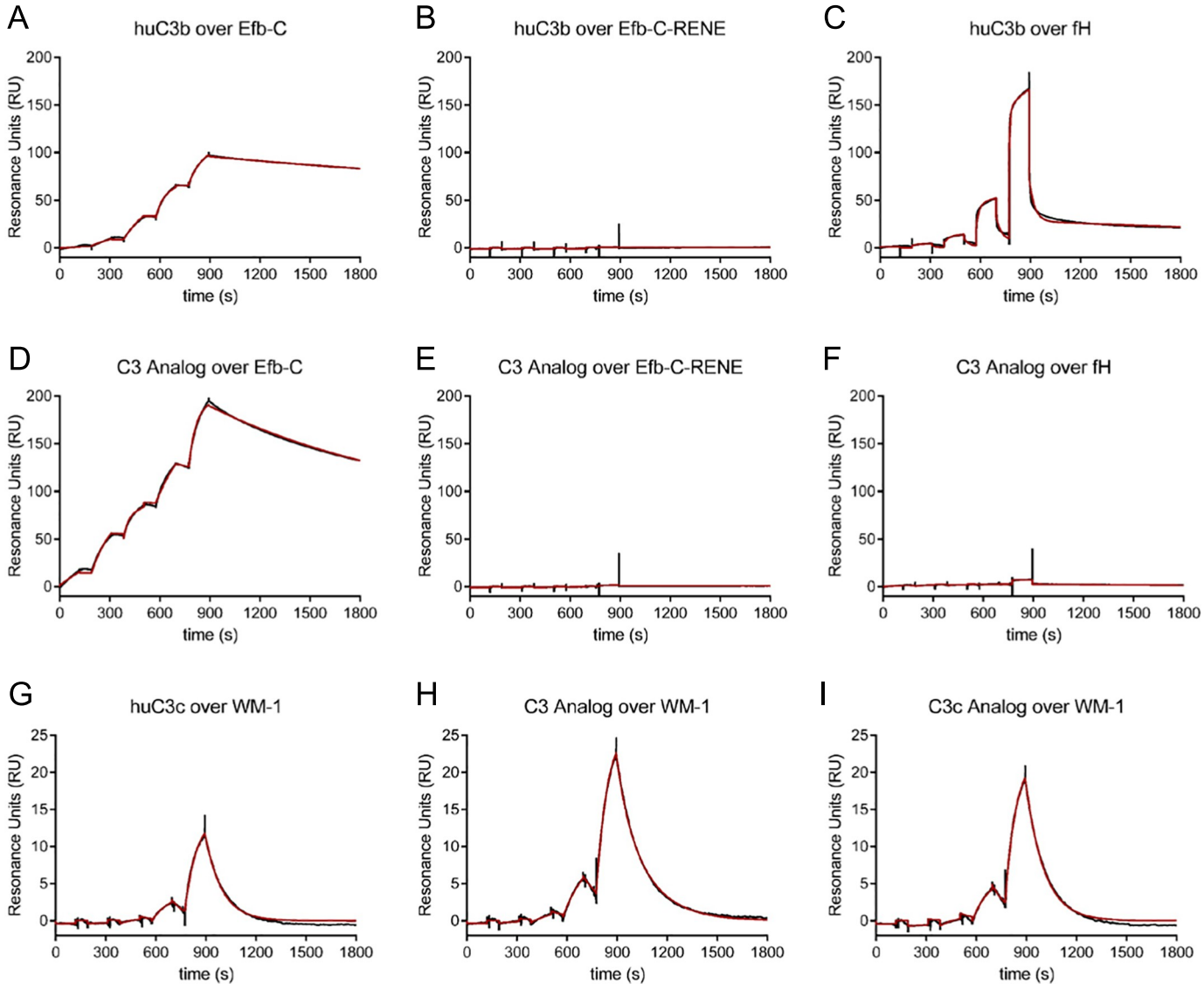

Fig. 6. Evaluation of the conformational state of human C3 and C3c analogs by their ligand binding profiles.
Surface plasmon resonance was used to compare the ligand binding profiles of the human C3 analog and its C3c-like state with control proteins native human C3b (i.e. huC3b) and C3c (i.e. huC3c). (panels A-C) Single-cycle, reference corrected sensorgrams (black lines) and their corresponding fits (red lines) obtained following injection of a concentration series of human C3b over surfaces consisting of (A) *S. aureus* Efb-C, (B) its non-functional double mutant Efb-C-RENE, and (C) purified human complement factor H. (panels D-F) A similar set of experiments to those presented in panels A-C, except that a concentration series of the human C3 analog was injected over surfaces consisting of (D) Efb-C, (E) Efb-C-RENE, and (F) purified human complement factor H. (panels G-I) Single-cycle, reference corrected sensorgrams (black lines) and their corresponding fits (red lines) obtained following injection of a concentration series of (G) native human C3c, (H) the human C3 analog, and (I) the human C3c analog, over a surface consisting of immobilized monoclonal antibody WM-1. (For interpretation of the references to colour in this figure legend, the reader is referred to the web version of this article.)

efficient TEV protease recognition site (Kapust et al., 2002), the residue immediately following the substrate P1′ site is Cys-1364. The sidechain of Cys-1364 forms a disulfide bond with the sidechain of Cys-1495, presumably stabilizing the eighth macroglobulin-like domain (MG8; Figs. S1 and S2). We suspect that this localized physical restriction interfered with substrate binding or efficient catalysis by the MBP-TEV fusion protein used in these studies. We favor this explanation over one based upon an argument of global steric hindrance, since the structure of C3b shows that the polypeptide chain both N- and C-terminally to the CUB-TED region lies in very close proximity to the “key ring”, yet the TEV site introduced at positions Glu-935 to Gly-941 was efficiently processed by TEV (Fig. 5 and Fig. S2B). It remains possible that TEV cleavage at this last position could still occur if more favorable reaction conditions were employed. In this regard, TEV protease is a thiol protease that requires the presence of reducing agent for maximal activity. Unfortunately, the presence of extensive intra- and inter-chain disulfide bonding in our C3 analog precluded inclusion of reagents like 2-mercaptoethanol or 1,4-dithiothreitol in our TEV activation reaction. The optimization of reaction conditions to include more mild reducing agents (e.g. varying ratios of reduced and oxidized glutathione) could be explored in future work, as could studies on similar C3 analogs designed to be cleaved by highly-specific, non-thiol proteases (e.g. Rhinovirus 3C-protease).

Despite the fact that TEV cleavage at the Glu-1357 to Ser-1363 site was unsuccessful, we determined that adventitious proteolysis in the area of Met-1353 to Tyr-1360 allowed for complete removal of the CUB-TED region from the truncated C3 analog. The resulting protein migrated as an ~115 kDa species in electrophoresis studies (Fig. 5) and retained ligand-binding properties analogous to human C3c (Figs. 6 and 7 and Table 1). Together, these data confirmed that the purified

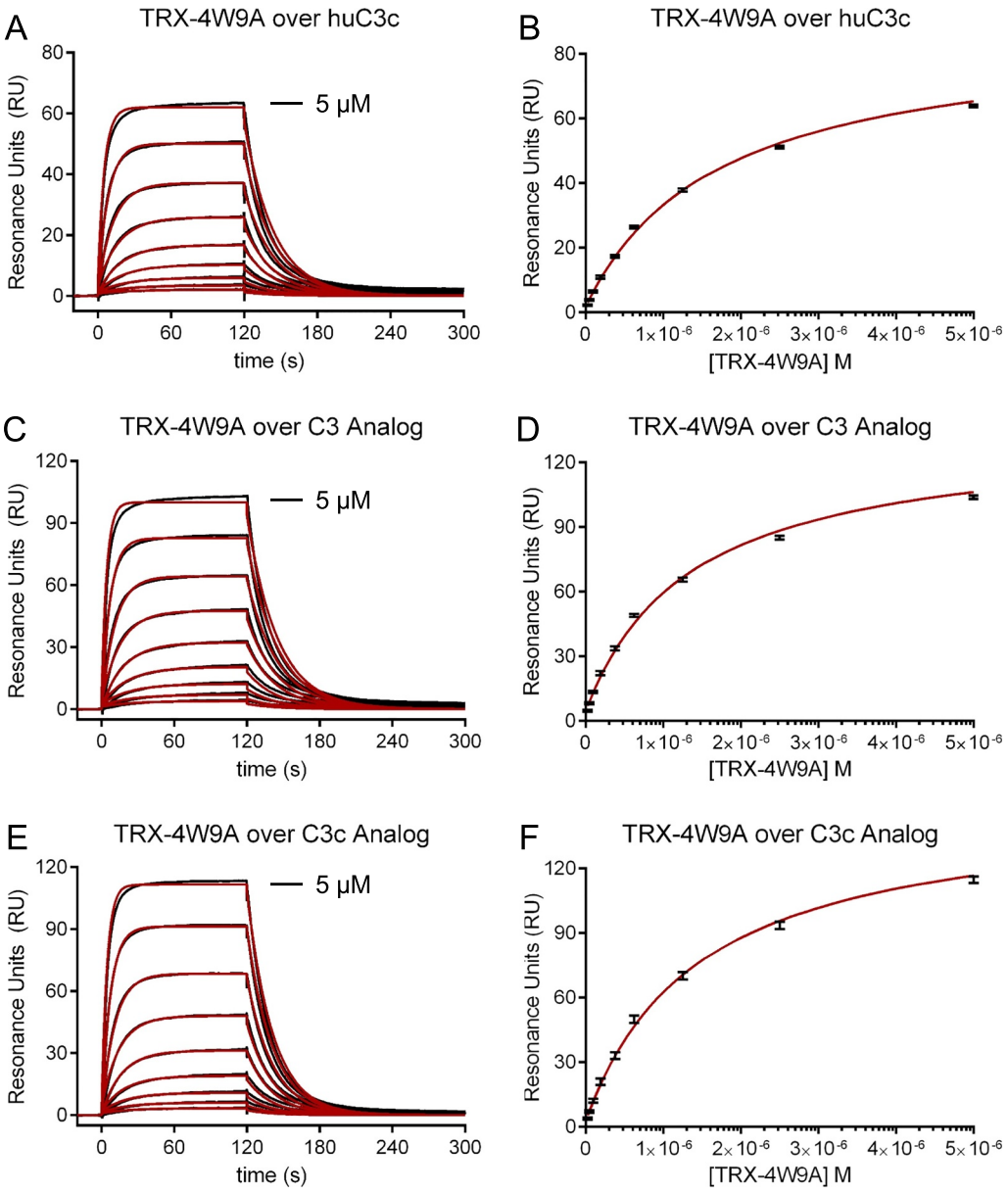

Fig. 7. Both the human C3 analog and its C3c-like activation product bind to the C3/b/c ligand TRX-4W9A.
The interaction of soluble TRX-4W9A fusion protein to immobilized human C3 analog, its C3c-like counterpart, and purified human C3c (i.e. huC3c) was analyzed by Surface Plasmon Resonance. (A) Representative reference corrected sensorgrams obtained following injection of a dilution series of TRX-4W9A over the human C3 analog (black lines) and their corresponding fits to a 1:1 model (red lines). (B) Approach to equilibrium analysis for the experiment shown in panel A. The response level prior to injection stop for three replicate injections (black error bars) at each concentration was plotted and fit to a Langmuir binding isotherm (red lines). (C) Representative reference corrected sensorgrams obtained following injection of a dilution series of TRX-4W9A over the human C3c analog (black lines) and their corresponding fits to a 1:1 model (red lines). (D) Approach to equilibrium analysis for the experiment shown in panel C. The response level prior to injection stop for three replicate injections (black error bars) at each concentration was plotted and fit to a Langmuir binding isotherm (red lines). (E) Representative reference corrected sensorgrams obtained following injection of a dilution series of TRX-4W9A over purified human C3c (black lines) and their corresponding fits to a 1:1 model (red lines). (F) Approach to equilibrium analysis for the experiment shown in panel E. The response level prior to injection stop for three replicate injections (black error bars) at each concentration was plotted and fit to a Langmuir binding isotherm (red lines). (For interpretation of the references to colour in this figure legend, the reader is referred to the web version of this article.)

Table 1
Rate and dissociation constants for TRX-4W9A binding obtained by surface plasmon resonance[a].

Ligand	k_{on} (M^{-1} s^{-1})	k_{off} (s^{-1})	K_D (nM)	Rmax (RU)
C3 analog	$4.17 \pm 0.14 \times 10^4$	$3.99 \pm 0.02 \times 10^{-2}$	956 ± 26	113 ± 10
C3c analog	$4.62 \pm 1.53 \times 10^4$	$5.98 \pm 2.33 \times 10^{-2}$	1280 ± 96	138 ± 5
Human C3c	$3.09 \pm 0.12 \times 10^4$	$4.18 \pm 0.14 \times 10^{-2}$	1350 ± 8	73.5 ± 14

[a] All values are reported as the mean ± standard deviation for three independent injection series over the same biosensor surface.

activation product had the structural and functional properties of C3c, but without the C-terminal C345c domain. This was the outcome that we intended. While there is room for improvement on what we have done thus far, we believe that our approach could be further refined and adapted for future work. For example, we chose to mutate Cys-1010 to eliminate the possibility for thioester formation in our C3 analogs. This mutation is beneficial in certain cases, as it eliminates the formation of disulfide-linked homodimers upon activation of C3. In other cases, the exposure of a unique cysteine sidechain can be used to modify the protein for downstream applications, in particular protein-protein interaction studies (Garcia et al., 2017; Garcia et al., 2012; Ricklin et al., 2009). Thus, we envision future functional studies involving a C3 analog which lacks the C345c domain, but retains its thioester group. Separately, complement component C4 shares key structural with features C3, as well as several analogous functional properties relevant to the Classical and Lectin Pathways (Ricklin et al., 2010). We expect that C4 analogs could be designed, expressed, and purified so that site-specific digestion by an exogenous enzyme like TEV protease would produce various C4 activation fragments and/or targeted deletion mutants thereof. Finally, C3b exists in an equilibrium distribution of

open and closed conformers with apparently distinct functional profiles (Chen et al., 2010), and the same is likely true for C4b as well (Woehl et al., 2017). Thus, we believe it should be possible to use recombinant systems such as those described here to generate targeted mutations in C3 and/or C4 that selectively trap the activated form of these proteins in one conformational state or another. This should facilitate structure/function analyses of these conformers in isolation, and ultimately provide a more complete understanding of these central complement components.

Acknowledgments

The authors wish to acknowledge helpful discussions with Dr. Samuel Bouyain (School of Biological Sciences, University of Missouri-Kansas City) and Dr. Brandon L. Garcia (East Carolina University School of Medicine) during various stages of this project. This work was funded by grants AI113552, AI111203, and NS104767 from U.S. National Institutes of Health to B.V.G.

Appendix A. Supplementary data

Supplementary data to this article can be found online at https://doi.org/10.1016/j.jim.2019.07.005.

References

Chen, H., et al., 2010. Allosteric inhibition of complement function by a staphylococcal immune evasion protein. Proc. Natl. Acad. Sci. U. S. A. 107, 17621–17626.
Dodds, A.W., 1993. Small-scale preparation of complement components C3 and C4. Methods Enzymol. 223, 46–61.
Forneris, F., et al., 2010. Structures of C3b in complex with factors B and D give insight into complement convertase formation. Science 330, 1816–1820.
Garcia, B.L., et al., 2010. Molecular basis for complement recognition and inhibition determined by crystallographic studies of the staphylococcal complement inhibitor (SCIN) bound to C3c and C3b. J. Mol. Biol. 402, 17–29.
Garcia, B.L., et al., 2012. Diversity in the C3b contact residues and tertiary structures of the staphylococcal complement inhibitor (SCIN) protein family. J. Biol. Chem. 287, 628–640.
Garcia, B.L., et al., 2013. A structurally dynamic N-terminal Helix is a key functional determinant in staphylococcal complement inhibitor (SCIN) proteins. J. Biol. Chem. 288, 2870–2881.
Garcia, B.L., et al., 2017. Identification of C3b-binding small-molecule complement inhibitors using cheminformatics. J. Immunol. 198, 3705–3718.
Gros, P., Milder, F.J., Janssen, B.J.C., 2008. Complement driven by conformational changes. Nat. Rev. Immunol. 8, 48–58.
Hajishengallis, G., Reis, E.S., Mastellos, D.C., Ricklin, D., Lambris, J.D., 2017. Novel mechanisms and functions of complement. Nat. Immunol. 18, 1288–1298.
Hammel, M., et al., 2007a. A structural basis for complement inhibition by *Staphylococcus aureus*. Nat. Immunol. 8, 430–437.
Hammel, M., et al., 2007b. Characterization of Ehp: a secreted complement inhibitory protein from *Staphylococcus aureus*. J. Biol. Chem. 202, 30051–30061.
Harboe, M., Ulvund, G., Vien, L., Fung, M., Mollnes, T.E., 2004. The quantitative role of alternative pathway amplification in classical pathway induced terminal complement activation. Clin. Exp. Immunol. 138, 439–446.
Janssen, B.J.C., et al., 2005. Structures of complement component C3 provide insights into the function and evolution of immunity. Nature 437, 505–511.
Janssen, B.J.C., Christodoulidou, A., McCarthy, A., Lambris, J.D., Gros, P., 2006. Structure of C3b reveals conformational changes underlying complement activity. Nature 444, 213–216.
Janssen, B.J., Halff, E.F., Lambris, J.D., Gros, P., 2007. Structure of compstatin in complex with complement component C3c reveals a new mechanism of complement inhibition. J. Biol. Chem. 282, 29241–29247.
Kajander, T., et al., 2011. Dual interaction of factor H with C3d and glycosaminoglycans in host-nonhost discrimination by complement. Proc. Natl. Acad. Sci. U. S. A. 108, 2897–2902.
Kapust, R.B., Tozser, J., Copeland, T.D., Waugh, D.S., 2002. The P1' specificity of tobacco etch virus protease. Biochem. Biophys. Res. Commun. 294, 949–955.
Katragadda, M., Magotti, P., Sfyroera, G., Lambris, J.D., 2006. Hydrophobic effect and hydrogen bonds account for the improved activity of a complement inhibitor, compstatin. J. Med. Chem. 49, 4616–4622.
Keightley, J.A., Shang, L., Kinter, M., 2004. Proteomic analysis of oxidative stress-resistant cells: a specific role for aldose reductase overexpression in cytoprotection. Mol. Cell. Proteomics 3, 167–175.
Leahy, D.J., Dann 3rd, C.E., Longo, P., Perman, B., Ramyar, K.X., 2000. A mammalian expression vector for expression and purification of secreted proteins for structural studies. Protein Expr. Purif. 20, 500–506.
Rawal, N., Pangburn, M.K., 2000. Functional role of the non-catalytic subunit of the complement C5 convertase. J. Immunol. 164, 1379–1385.
Rawal, N., Pangburn, M.K., 2001. Formation of high-affinity C5 convertases of the alternative pathway of complement. J. Immunol. 166, 2635–2642.
Rawal, N., Pangburn, M.K., 2003. Formation of high affinity C5 convertase of the classical pathway of complement. J. Biol. Chem. 278, 38476–38483.
Ricklin, D., Lambris, J.D., 2013. Compement in immune and inflammatory disorders: pathophysiological mechanisms. J. Immunol. 190, 3831–3838.
Ricklin, D., et al., 2009. A molecular insight into complement evasion by the staphylococcal complement inhibitor protein family. J. Immunol. 183, 2565–2574.
Ricklin, D., Hajishengallis, G., Yang, K., Lambris, J.D., 2010. Complement: a key system for immune surveillance and homeostasis. Nat. Immunol. 11, 785–797.
Ricklin, D., Reis, E.S., Mastellos, D.C., Gros, P., Lambris, J.D., 2016. Complement component C3 - the "swiss army knife" of innate immunity and host defense. Immunol. Rev. 274, 33–58.
Rooijakkers, S.H., et al., 2009. Structural and functional implications of the alternative complement pathway C3 convertase stabilized by a staphylococcal inhibitor. Nat. Immunol. 10, 721–727.
Sahu, A., Lambris, J.D., 2001. Structure and biology of complement protein 3, a connecting link between innate and acquired immunity. Immunol. Rev. 180, 35–48.
Summers, B.J., et al., 2015. Identification of Peptidic inhibitors of the alternative complement pathway based on Staphylococcus aureus SCIN proteins. Mol. Immunol. 67, 193–205.
Whitehead, A.S., Sim, R.B., Bodmer, W.F., 1981. A monoclonal antibody against human complement component C3: the production of C3 by human cells in vitro. Eur. J. Immunol. 11, 140–146.
Wiesmann, C., et al., 2006. Structure of C3b in complex with CRIg gives insights into regulation of complement activation. Nature 444, 217–220.
Woehl, J.L., Ramyar, K.X., Katz, B.B., Walker, J.K., Geisbrecht, B.V., 2017. The structural basis for inhibition of the classical and Lectin complement pathways by S. aureus extracellular adherence protein. Protein Sci. 26, 1595–1608.
Wu, J., et al., 2009. Structure of complement fragment C3b-factor H and implications for host protection by complement regulators. Nat. Immunol. 10, 728–733.
Xue, X., et al., 2017. Regulator-dependent mechanisms of C3b processing by factor I allow differentiation of immune responses. Nat. Struct. Mol. Biol. 24, 643–651.
Yang, K., et al., 2013. CMAP: complement map database. Bioinformatics 29, 1832–1833.